Desalination and Water Treatment
www.deswater.com

doi:10.5004/dwt.2018.23262

135 (2018) 268–278
December

Evaluation of the adsorption potential of iron and manganese oxide immobilized sand for the removal of Cs(I) and Sr(II) from aquatic environment

Lalhmunsiama[a], Munui Kim[a], Yi-Yong Yoon[a,*], Jae-Gyu Kim[a], Suk Soon Choi[b], Sang-Il Choi[c], Seung-Mok Lee[a,*]

[a]*Department of Environmental Engineering, Catholic Kwandong University, Gangneung 25601, Korea, email: lhsiama27@gmail.com (Lalhmunsiama), monyangi@naver,com (M. Kim), yoonyy@cku.ac.kr (Y.-Y. Yoon), dkc10221@hanmail.net (J.-G. Kim), Tel. +82-10-8891-7635, Fax +82-33-642-7635, email: leesm@cku.ac.kr (S.-M. Lee)*
[b]*Department of Biological and Environmental Engineering, Semyung University, Jecheon 27136, Korea, email: sschoi@semyung.ac.kr (S. S. Choi)*
[c]*Department of Environmental Engineering, Kwangwoon University, Seoul 01897, Korea, email: sichoi@kw.ac.kr (S.-I. Choi)*

Received 16 April 2018; Accepted 9 October 2018

ABSTRACT

In this study, iron oxide immobilized sand (IIS) and manganese oxide immobilized sand (MIS) were prepared by impregnation method and employed for the removal of Cs(I) and Sr(II) from aqueous solutions. The characterizations of IIS and MIS along with the bare sand were performed with the help of SEM-EDX, FT-IR and XRD analyses. The amount of iron and manganese loaded on the sand surface were 4.52 mg/g and 1.57 mg/g, respectively. Further, the stability test showed that iron/manganese oxide particles were strongly aggregated on the sand surface. An enhanced uptake of Cs(I) and Sr(II) were shown by IIS and MIS compared to the bare sand. The Langmuir monolayer adsorption capacity of IIS were found to be 5.102 and 1.324 mg/g for Cs(I) and Sr(II), respectively; whereas the MIS showed 2.409 and 1.277 mg/g for Cs(I) and Sr(II), respectively. The time dependent adsorption data follows pseudo second order kinetic better than pseudo first order kinetic model. The presence of other heavy metals caused a decreased in the removal of Cs(I)/Sr(II) by IIS/MIS. The effect of ionic strength studies indicate that Cs(I) and Sr(II) are weakly bound through electrostatic attraction and form outer sphere complexes on the surfaces of IIS and MIS. Further, the breakthrough curves were obtained through fixed bed column experiments and the loading capacity of the column packed with IIS or MIS were evaluated.

Keywords: Radio toxic ions; Natural sand; Removal; Kinetic; Fixed bed column

1. Introduction

Enhance use of radioactive elements in nuclear power plant in order to afford high energy requirement in turn produced large amount of radioactive waste. Moreover, nuclear weapon testing and the accidents occurred in nuclear power plants due to earthquake and tsunami extensively generate radioactivity to the environment. Therefore, radioactive contamination has become a crucial environmental issue in many countries [1]. Cesium is one of the fission products frequently present in radioactive liquid effluents and it is considered as the most hazardous element to the environment [2]. ^{134}Cs and ^{137}Cs are the major fission products having long half-lives of 2.06 y and 30.2 y, respectively [3]. ^{137}Cs has received more concern due to its abundance and gamma radiation emission [4]. Moreover, Cs-137 is reported as a major source of radiation and heat in the high-level radioactive waste [5,6]. Due to high water solubility, cesium can easily enter human body and possibly caused an internal hazard such as cancer. Moreover, due to similarities in chemical properties with sodium and potassium, cesium has high tendency to incorporate to terrestrial and aquatic habitats, so it is a potential toxic contaminant

*Corresponding author.

in water [7]. Strontium is another important radionuclide, which is found in significant amount in the spent fuel of nuclear reactor and the fallout from nuclear weapons test [8]. ^{90}Sr and ^{89}Sr are two important radio-strontium mainly generated from the nuclear fission of ^{235}U and ^{239}Pu, having half-lives of 28.6 y and 53 d respectively [9]. ^{90}Sr mainly present as the Sr^{2+} ion which could replace calcium ions and increase the possibility of leukemia and other diseases in the human body [10,11]. These radio toxic pollutants are potentially destructive to living beings even at diminutive levels. Therefore, the attenuation of toxic cesium and strontium from the human environment is highly necessary.

In order to abate the radioactive contamination in aquatic environment, different types of technique such as membrane separation [12], reverse osmosis filtration [13], adsorption [14], electro-coagulation process [1], electro-deionisation [15], ion exchange [16] were investigated for the removal of Cs or Sr from aqueous media. Adsorption is found to be an appropriate technique to abate radioactive contamination due to its low cost, versatile and easy operation [17]. Different types of adsorbents including magnetic graphene oxides [18], zeolites [19], mesoporous silica [20], *Azollafiliculoides* [21], Egyptian soils [22], sericite and activated sericite [3,23] were reported to remove cesium and strontium from aqueous solutions. Furthermore, the metal-organic framework-based materials [24] and poly(amidoxime) modified reduced graphene oxide [25] were observed to be superior adsorbents for the capture of radioactive metal ions.

Sand is commonly utilized as filter medium in water purification system due to its natural abundance, low cost and chemical stability. Previously, it was observed that, during the wastewater treatment, iron and manganese present in wastewater are incorporated on the sand surface in their oxides form. This material had been found to be fairly efficient for the adsorption of several toxic heavy metals due to their selectivity toward several metal ions [26]. Moreover, use of iron and manganese in wastewater treatment has advantages since they are abundant in nature and non toxic to the environment [27,28]. Therefore, the surface modification of sand by incorporating iron or manganese could facilitate the suitability of natural sand for the removal of various toxic metal ions including radio toxic ions from aqueous solutions. The successful utilization of iron or manganese oxide modified sand for the adsorption of heavy metals [29–32], arsenic [33], antimony [34], dyes [35] were reported. However, the investigation about the application of these materials in the attenuation of radio toxic ions is limited. So it is interesting to study the efficiency of iron and manganese coated sand for the removal of Cs(I) and Sr(II). Therefore, the present study aims to incorporate iron or manganese oxide onto locally available natural sand by simple impregnation process. The materials were characterized and further employ for the removal of two radio toxic ions, i.e., Cs(I) and Sr(II) from aqueous solutions.

2. Experimental

2.1. Materials and chemicals

The bare sand was collected from the riverbank of 'Tlawng' at Sairang site, Mizoram, India. The sand was soaked in the diluted acid overnight to remove any impurities. Then, it was rinsed for several time using distilled water and kept inside the drying oven for further use. The size of sand is 0.5–1.0 mm. $Fe(NO_3)_3{\cdot}9H_2O$ and $Mn(NO_3)_2.6H_2O$ were obtained from Kanto Chemicals Co. Inc., and Junsei Chemical Co. Ltd., Japan, respectively. Cesium chloride was procured from Kanto Chemicals Co. Inc., Japan, whereas the strontium nitrate was procured from Deajung Chemicals and Metals Co. Ltd., Korea. All other chemicals were AR grade and the water used in all experiments was distilled by the Milli-pore water purification system.

2.2. Preparation of iron oxide immobilized sand (IIS) and manganese oxide immobilized sand (MIS)

100 mL of iron nitrate solution (0.05M) was prepared and the solution pH was maintained at 8.5. The solution was kept in a round bottom flask and then 50 g of sand was added in the solution. The flask containing the mixture was fixed in a rotary evaporator and the rotating speed was 30 rpm at 60°C. The vacuum pump was applied slowly and about 90% of water was removed. The remaining mixture was kept at 90°C inside the oven to dry completely. Thereafter, the solid sample was kept at 120°C (2 h) to stabilize the immobilized iron-oxide particles. After the sample was cooled down to room temperature, it was washed with pure water and then again dried at 70°C. The modified sand is named as iron oxide immobilized sand (IIS). The same procedure was repeated using manganese nitrate solution to obtain manganese oxide immobilized sand (MIS).

2.3. Characterization

The ultra-high resolution scanning electron microscope (SEM) with energy dispersive X-ray spectroscopy (EDX) system (FE-SEM SU-70, Hitachi, Japan) was used for obtaining the micro graph and elemental compositions of bare sand, IIS and MIS. The X - ray diffraction patterns of these solids were collected using XRD machine (X'Pert PRO MPD: PAN alytical, Netherland). Moreover, Fourier transform infrared spectroscopy (FT-IR; Model: Tensor 27, Bruker, USA) was employed to identify the functional groups present on the surface of bare sand as well as modified sand.

2.4. Determination of iron and manganese content and stability of IIS and MIS samples

The iron and manganese content in the IIS and MIS as well as bare sand were determined by US EPA 3050B method and the amount of iron or manganese particles loaded onto the sand surface were determined. Moreover, the stability tests for immobilized iron or manganese particles were conducted within pH 2.0 to 10.0. In this process, 100 mL of water were kept in several polyethylene bottles and the pH of these water were adjusted to pH 2.0 to 10.0 by the addition of drops of 0.1 mol/L HNO_3 and 0.1 mol/L NaOH solutions. 0.25 g of sand or IIS or MIS was introduced in a three series of pH. The bottles were kept in automatic shaker at 25°C for 24 h. The samples were filtered using membrane filter (0.45 μm) and the total iron or manganese concentrations were analyzed using atomic absorption spectrometer (AAS; Model: AA240FS, Varian).

2.5. Batch experiments

Batch experiments were performed to study the effect of solution pH, initial Cs(I)/Sr(II) concentrations, contact time, and presence of heavy metal ions and ionic strength in the removal of Cs(I) and Sr(II) using IIS and MIS solids. In this study, 50 ml of Cs(I)/Sr(II) solution were taken in polyethylene bottles and the pH of solutions were adjusted using 0.1 mol/L HNO_3/NaOH solution. Then, 0.25 g of the adsorbent was added to each bottle i.e., 5.0 g/L for all batch experiments. The solution mixture was kept inside the automatic shaker with rotating speed of 150 rpm at 25 ± 1°C for 12 h to achieve the adsorption equilibrium. After the adsorption process was completed, the solutions were filtered by membrane filter (0.45 µm) and the concentration of Cs(I)/Sr(II) were analyzed using the Fast Sequential Atomic Absorption Spectrometer (Model: AA240FS, Varian, Australia).

The effect of initial concentration was performed within the initial concentration between 4.0 and 28.0 mg/L for Cs(I) and between 1.0 to 18.0 mg/L for Sr(II) at constant pH 5.0. The adsorption data obtained within a wide range of initial concentration are further utilized for Langmuir and Freundlich adsorption isotherm studies. The effect of contact time was studied by measuring the extent of adsorption at various intervals of time within 12 h. The experiments were performed at pH 5.0 keeping the initial concentration of Cs(I) and Sr(II) at 10.13 mg/L and 6.99 mg/L, respectively. The kinetic data collected were utilized to fit into the pseudo-first order and pseudo-second order kinetic model. Furthermore, the effect of presence of other heavy metal ions such as Cd(II), Cu(II), Mn(II), Pb(II) and Sr(II)/Cs(I) were evaluated. The concentration of heavy metal ions were 50 mg/L and the initial concentration of Cs(I) and Sr(II) are 10.32 and 6.64 mg/L for, respectively. In addition, the effect of ionic strength in the removal of Cs(I) and Sr(II) were conducted by increasing the concentration of $NaNO_3$ from 0.001 to 0.1 mol/L. The initial concentration of Cs(I) and Sr(II) are 10.5 and 7.8 mg/L respectively, and the solutions pH's were maintained at 5.0.

2.6. Fixed-bed column adsorption

The removal behavior of Cs(I) and Sr(II) by IIS and MIS was studied in fixed-bed column system using a glass column with 1 cm inner diameter and 10 cm length. The IIS or MIS (1.0 g) was firmly packed inside the column using glass beads. The Cs(I)/Sr(II) solutions (Cs(I): ~10 mg/L, Sr(II): ~5 mg/L and pH 5.0)was pump upward through the column at a flow rate of 1.00 mL/min. The high-pressure liquid chromatograph, Acuflow Series II was used for maintaining the flow rate and the effluent samples were collected by Spectra/Chrom CF-2 fraction collector. The final concentration of Cs(I)/Sr(II) were analyzed using AAS.

3. Results and discussion

3.1. Characterization of materials

The SEM micro graph of bare sand, IIS and MIS solids are displayed in Figs. 1a–c. The surface morphology of the bare sand was relatively smooth and several micro pores were visible on sand surface (Fig. 1a). The surface images of IIS (Fig. 1b) and MIS (Fig. 1c) showed that reasonable amount of iron or manganese oxides were incorporated onto the sand surface as small sized particles and increase heterogeneity on the sand surface. Moreover, it can be seen from the SEM image that the small pores present on the bare sand surface were partly filled with the iron or manganese particles.

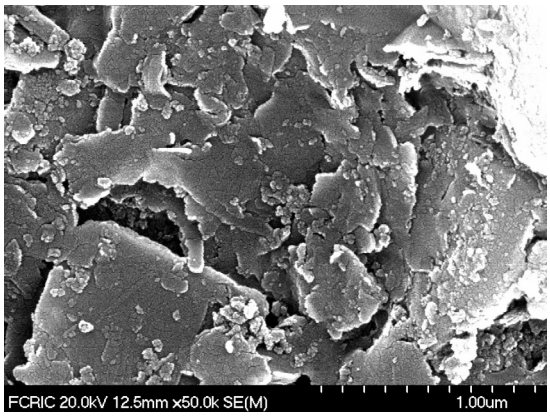

(a)

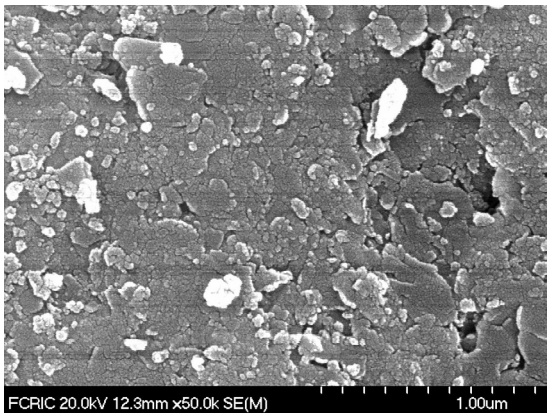

(b)

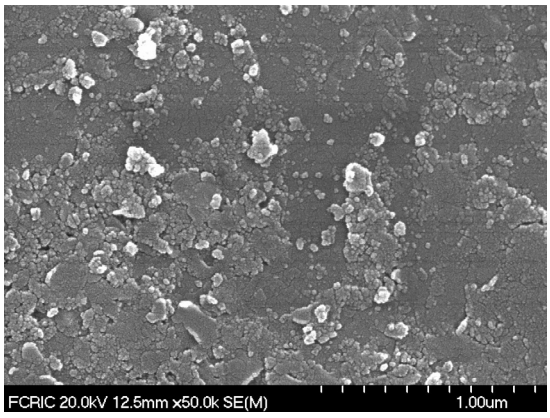

(c)

Fig. 1. SEM micro graph of (a) Sand (b) IIS and (c) MIS samples.

The XRD diffraction pattern of bare sand, IIS and MIS solids were obtained and are graphically presented in Fig. 2. All the three samples show similar diffraction peak; but the relative intensities of the peaks differ from one sample to another. The major peak obtained at 2θ values of 26.5° indicates the presence of silica as main components in these samples. The IIS sample show characteristic peaks of Fe_2O_3 at 36.6° and 51° [36]. Further, distinguish peaks obtained at 36.7° and 42.5° in MIS corresponds to 110 and 11(–2) crystal planes of δ-MnO_2 [37].

Furthermore, the functional groups present in the sand, IIS and MIS samples were distinguished by FT-IR analysis. The IR spectra within the frequency ranges between 4000 and 400 cm^{-1} are graphically shown in Fig. 3. The predominant peaks at 1045, 1010 and 780 cm^{-1} were ascribed to Si-O-Si asymmetric and symmetric stretching vibrations [35]. The peak shown at 685 cm^{-1} due to symmetrical bending vibrations of Si-O confirms the presence of SiO_2 and quartz in crystal form [38,39]. A small peak obtained at around 910 cm^{-1} for all the three samples is attributed to Si-O stretch mode [40]. The bands appearing at 460 cm^{-1} were ascribed to Si-O asymmetrical bending vibrations. The broad absorption bands present at 3447 cm^{-1} were due to –OH stretching vibration of absorbed water molecules [39], while the distinguish peak at 1635 cm^{-1} were due to bending vibrations –OH group [41]. The stretching band observed at 3625 cm^{-1} in case of bare sand was perhaps, due to the water present within the micro pores of sand sample [42].

3.2. Iron and manganese content and Stability of IIS and MIS samples

The amount of iron and manganese present in the samples were determined by USEPA 3050B method. The amount of iron content in bare sand and IIS samples were determined to be 19.81 mg/g and 24.33 mg/g, respectively. The manganese content in bare sand and MIS were relatively low and found to be 0.27 mg/g and 1.84 mg/g, respectively. Therefore, the amount of iron and manganese loaded on the sand surface were 4.52 mg/g and 1.57 mg/g, respectively.

Furthermore, the stability of IIS and MIS samples were investigated and the results are given in Fig. 4. The iron oxide particles were strongly aggregated on the sand surface within pH 3 and 10. Similarly, the manganese oxide particles were found to be stable within pH 4 and 10.These results indicate that iron particles were slightly stable than manganese particles. The iron particles were observed to desorbed only at pH 2.0, whereas a very small amount of manganese particles start to desorbed from pH 4.0. Therefore, these results suggest the possible use of IIS and MIS materials with in a wide pH range in wastewater treatment. The similar stability was previously observed for the iron or manganese immobilized on the activated carbons [43].

3.3. Batch adsorption studies

3.3.1. Effect of pH

The speciation studies has shown that cesium mostly exists as Cs(I) within the pH ranges between 2 and 10. Similarly, strontium also exists as Sr(II) within the same pH ranges; however, at pH 10, strontium has a little tendency to form $Sr(OH)^+$ [44]. On the other hand, changes in solution pH greatly influences the surface charge of the adsorbents; thus, pH must be one the most influential parameters in Cs(I) and Sr(II) removal from the aqueous solutions [23].

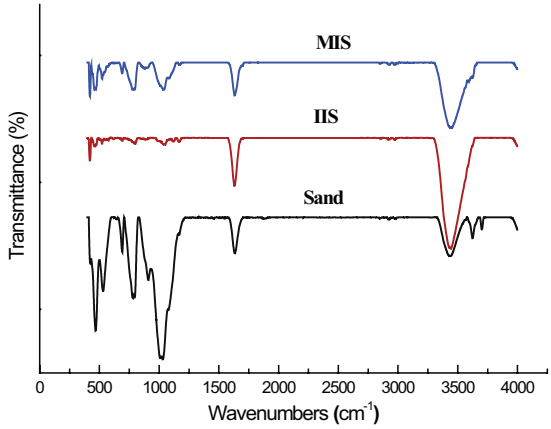

Fig. 3. FT-IR spectra obtained for bare sand, IIS and MIS.

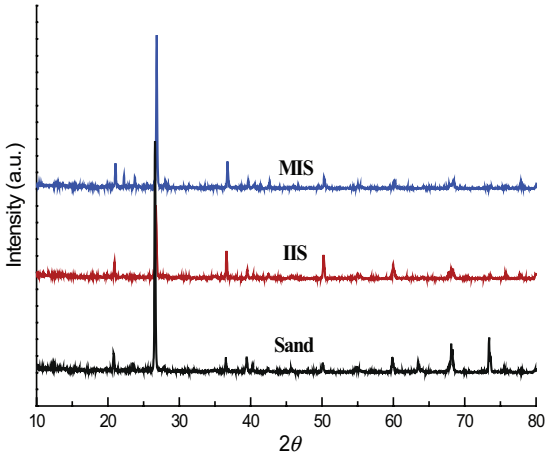

Fig. 2. XRD patterns of bare sand, IIS and MIS.

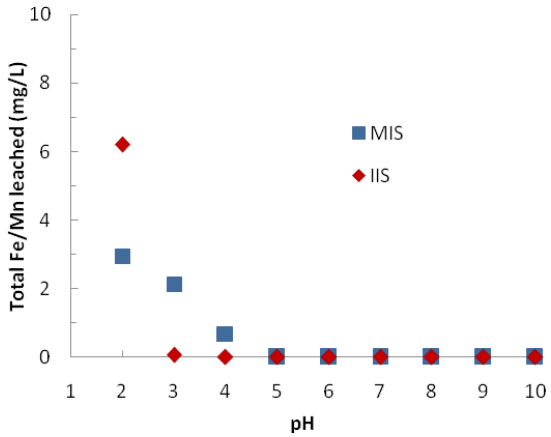

Fig. 4. Stability of iron or manganese immobilized sand as a function of solution pH.

Therefore, Cs(I) and Sr(II) adsorption experiments were conducted varying the initial solution pH between 2.0 and 10.0 and the initial Cs(I)/Sr(II) concentrations were approximately 10.0 mg/L. As shown in Fig. 5, the IIS and MIS showed significantly high percentage removal of Cs(I) as compared to the unmodified/bare sand. Moreover, the removal of Sr(II) was also improved to some extent for IIS and MIS samples. These results indicate the potential applicability of IIS and MIS for the removal of radio toxic Cs(I) and Sr(II) from the aqueous solutions. The percentage removal of these two radio toxic ions were notably lower in acidic medium which is caused by a strong competition between the Cs^{+}/Sr^{2+} ions and the excess hydrogen ions towards the same actives sites in IIS or MIS samples [45–47]. Moreover, an enhancement in the percentage removal of Cs(I) by the modified sand (i.e., IIS and MIS) at pH 2.0 and 3.0 is very small and almost same with the bare sand. Similarly, an improvement in Sr(II) removal using modified sand at pH 3.0 are very less and even the IIS showed the removal lower than the bare sand at pH 2.0. This might be due to the leaching of iron/manganese from the sand in acidic solutions. The percentage removal of Cs(I) by IIS and Sr(II) by IIS and MIS were considerably enhanced while increasing the initial pH from 2.0 to 4.0. Above pH 4.0, the percentage removal remained almost constant for both Cs(I) and Sr(II). However, the removal of Sr(II) was further improved at pH 10.0 which is possibly due to the formation of $Sr(OH)^{+}$ at this pH; therefore, the adsorption and co-precipitation of Sr(II) may occur simultaneously at this pH and consequently enhancing the uptake of Sr(II) [23]. The removal of Cs(I) by MIS showed a slightly different trend, the percent uptake constantly increases up to pH 6 and further increase in solution pH caused a slight increase up to pH 10.0. Therefore, the pH dependent study suggests that pH ranges from 5.0 to 8.0 must be suitable pH region for the removal of Cs(I) and Sr(II) using IIS/ MIS.

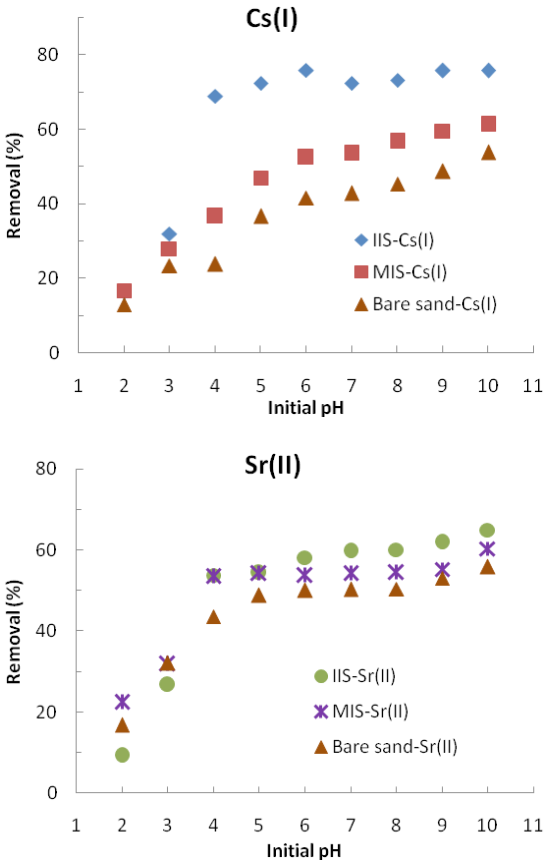

Fig. 5. Effect of pH in the adsorption of (a) Cs(I) and (b) Sr(II) by IIS and MIS (Initial [Cs(I)/Sr(II)]: ~10 mg/L, dose of the adsorbents: 5.0 g/L, contact time: 12 h).

3.3.2. Effect of initial concentration

In batch adsorption studies, the initial concentration of the adsorbate induces an active force to prevail over the mass transfer barrier at the interface of aqueous media and the adsorbent. Consequently, the adsorption is generally favoured by increasing the initial concentrations of the adsorbate [48]. The effect of initial concentrations was studied by varying the initial concentration between 4.78 to 27.74 of Cs(I) and 1.71 to 17.96 mg/L of Sr(II) at constant pH 5.0 and the results are graphically given in Fig. 6. The high percentage removals of Cs(I) and Sr(II) were observed at lower concentrations and slowly decreased while increasing initial concentration of Cs(I)/Sr(II). Briefly, the removal percentage of Cs(I) using IIS and MIS was found to be decreased from 88.45 to 66.84% and 78.28 to 37.79%, respectively, while increasing initial Cs(I) concentration from 4.78 to 27.74 mg/L. Moreover, the percentage removal of Sr(II) was lower than Cs(I), and the results showed that while the Sr(II) concentration increased from 1.71 to 17.96 mg/L the percentage of Sr(II) removal decreased from 79.06 to 32.73% and 63.68 to 28.28% using IIS and MIS samples, respectively.

The adsorption isotherm studies were performed with the concentration dependence adsorption data using Freundlich and Langmuir adsorption isotherm. The Freundlich isotherm equation is expressed as follows:

$$\log q_e = \frac{1}{n}\log C_e + \log K_F \tag{1}$$

where q_e (mg/g) denotes the amount of Cs(I)/Sr(II) adsorbed at equilibrium and C_e (mg/L) denotes the equilibrium concentration of Cs(I)/Sr(II). and K_F is the Freundlich constant and *1/n* is the heterogeneity factor [49]. The Langmuir isotherm equation [Eq. (2)] is taken as

$$\frac{C_e}{q_e} = \frac{1}{q_o K_L} + \frac{C_e}{q_o} \tag{2}$$

where C_e (mg/L) denotes the concentration of Cs(I)/Sr(II) at equilibrium and q_e (mg/g) denotes the amount of pollutant adsorbed at equilibrium; q_o (mg/g) represent the Langmuir maximum adsorption capacity of the pollutants and the Langmuir constant is denoted by 'K_L' [50,51]. The graphs plotted for Freundlich adsorption isotherms (*log* C_e vs. *log* q_e) and the Langmuir adsorption isotherms (C_e/q_e vs. C_e) are shown in Figs. 7a and b. The Freundlich and Langmuir constants are evaluated and summarized in Table 1. The coefficient of determination i.e., R^2 values indicates that the adsorption of Cs(I) on both IIS and MIS samples showed a better fit to Freundlich adsorption isotherm, whereas

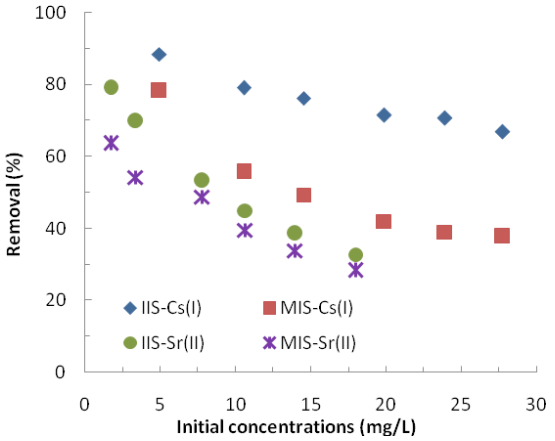

Fig. 6. Effect of initial concentrations in the adsorption of Cs(I) and Sr(II) by IIS and MIS from aqueous solutions (Initial [Cs(I)/Sr(II)]: 1.0–30.0 mg/L, pH: 5.0, dose of the adsorbent: 5.0 g/L, contact time: 12 h).

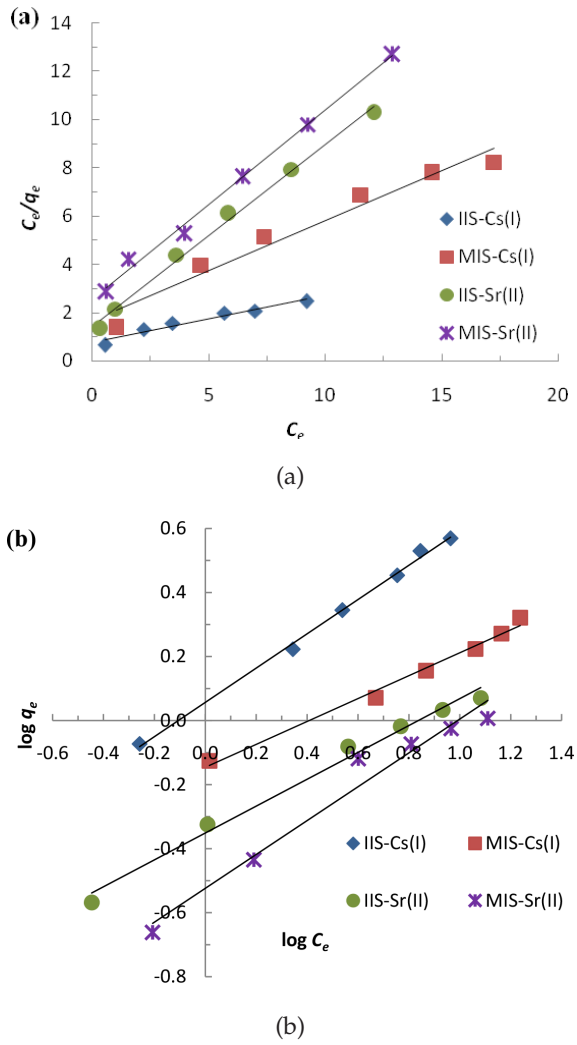

Fig. 7. Plots of (a) Langmuir adsorption isotherm (b) Freundlich adsorption isotherm for the removal of Cs(I) and Sr(II) using IIS and MIS.

Table 1
Langmuir and Freundlich constants and R^2 values obtained for the adsorption of Cs(I) and Sr(II) sing IIS and MIS

System	Langmuir			Freundlich		
	q_o (mg/g)	K_L (L/g)	R^2	$1/n$	K_F (mg/g)	R^2
IIS-Cs(I)	5.102	0.257	0.949	0.535	1.137	0.997
MIS-Cs(I)	2.409	0.249	0.959	0.357	1.396	0.988
IIS-Sr(II)	1.324	0.543	0.994	0.419	2.243	0.987
MIS-Sr(II)	1.277	0.309	0.993	0.528	3.334	0.966

the Sr(II) data fit well to Langmuir adsorption isotherm. This isotherm fitting results suggest that the adsorption behaviour of Sr(II) by IIS/MIS is different from Cs(I), and it can be assumed that Sr(II) ions were specifically adsorbed to the well defined and energetically equivalent sites only and possibly form monolayer on the surface of IIS/MIS [32]. The Langmuir adsorption capacity (q_o) obtained for Cs(I) are notably higher than Sr(II); whereas the Freundlich constant (K_F) values obtained for Sr(II) are larger than that of Cs(I). Similar results was previously reported for the adsorption of Sr(II) and Ba(II) using dolomite powder in which the Langmuir adsorption capacity of Ba(II) was significantly higher than Sr(II), but the Freundlich constant values of Sr(II) was found to be higher than Ba(II) [52]. Furthermore, the Freundlich constant (1/n) obtained for the IIS and MIS indicate the heterogeneous surface structure of solids employed for adsorption [53] and the higher values Langmuir constants (K_L) inferred that these solids (IIS and MIS) has good affinity towards Cs(I) and Sr(II)[29]. Previously reported Langmuir monolayer adsorption capacity of Cs(I)/Sr(II) of various adsorbents along with IIS and MIS are given in Tables 2a and 2b. The adsorption capacity of the adsorbent is significantly influence by the experimental factors including the initial concentration of pollutants, pH, temperature, ionic strength, etc., therefore, the actual comparison can be made if the experiments were performed under similar conditions only. However, as shown in Tables 2a and 2b, IIS and MIS possessed competitive adsorption capacity for Cs(I) and Sr(II) compared to other low cost adsorbents.

3.3.3. Effect of contact time

The percentage removal of Cs(I) and Sr(II) using IIS and MIS samples at various intervals of time were evaluated and the results are graphically shown in Fig. 8. Batch experiments were performed at pH 5.0 keeping the initial concentration of Cs(I) and Sr(II) at 10.13 mg/L and 6.99 mg/L, respectively. The Cs(I) and Sr(II) adsorption were relatively faster within the initial one hour and then retard beyond one hour of contact time. An apparent adsorption equilibrium was attained in 300 min and 360 min for Cs(I) and Sr(II), respectively.

The time dependent adsorption data were modelled with pseudo first order kinetic [Eq. (3)] and pseudo second order kinetic [Eq. (4)] models. The kinetic models were taken in its linear form as [64]:

Table 2a
Adsorption capacity of Cs(I) for various adsorbents obtained by Langmuir Isotherm

Material	Adsorption capacity (mg/g)	Reference
Prussian blue functionalized micro capsule	4.837	[54]
Immobilized NiHCF-sericite beads	13.877	[55]
Activated sericite	6.83	[3]
NiHCF-walnut shell	4.94	[56]
Akadama clay	4.5	[57]
Modified akadama clay	16.1	[57]
Pine cone	2.50	[58]
Iron(III) HCF-pine cone	5.77	[58]
Ain Oussera soil	4.31	[59]
Ceiling tiles	0.212	[60]
IIS	5.102	This study
MIS	2.409	This study

Table 2b
Adsorption capacity of Sr(II) for various adsorbents obtained by Langmuir Isotherm

Material	Adsorption capacity (mg/g)	Reference
Sericite	1.606	[23]
Activated sericite	1.547	[23]
Natural clinoptilolite	9.80	[61]
Magnetic Fe_2O_3 modified sawdust	12.59	[62]
Pecan shell based activated carbon	8.8	[63]
Dolomite powder	1.172	[52]
IIS-Sr(II)	1.324	This study
MIS-Sr(II)	1.277	This study

$$\ln\left(q_e - q_t\right) = \ln q_e - k_1 t \tag{3}$$

$$\frac{t}{q_t} = \frac{1}{k_2 q_e^2} + \frac{t}{q_e} \tag{4}$$

where q_e and q_t denotes the amount adsorbed of pollutants at equilibrium and at a given time t. The k_1 (1/min) is the rate constant of pseudo-first order, whereas k_2 (g/mg/min) is the pseudo-second order rate constant. The graphs plotted for pseudo-first order kinetic ($ln\ (q_e - q_t)$ vs t) and pseudo-first order and pseudo-second order kinetic (t/q_t vs t) are shown in Fig 9 (a and b). The adsorption rate constant (k_1 and k_2) and the maximum uptake of Cs(I) and Sr(II) at equilibrium (q_e) are evaluated and summarized in Table 3. The kinetic data obtained for Cs(I) and Sr(II) are fit well to pseudo-second order kinetic model than pseudo-first order kinetic model as indicated by the R^2 values. The experimental q_e values

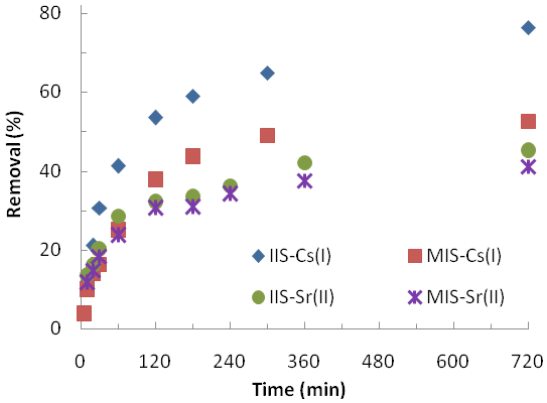

Fig. 8. Time dependent adsorption of Cs(I) and Sr(II) by IIS and MIS from aqueous solutions (Initial [Cs(I)/Sr(II)]: ~10 mg/L, pH: 5.0, dose of the adsorbent: 5.0 g/L, contact time: 12 h).

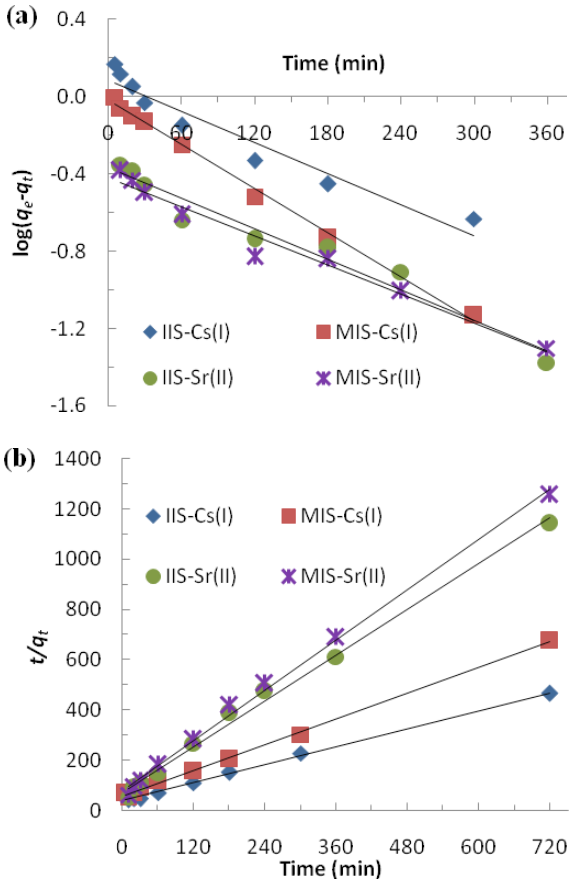

Fig. 9. Plots of (a) pseudo first order kinetic and (b) pseudo second order kinetic model for the removal of Cs(I) and Sr(II) using IIS and MIS.

obtained for the uptake of Cs(I) are 1.547 and 1.066 mg/g for IIS and MIS respectively, whereas the Sr(II) are 0.630 and 0.574 mg/g for IIS and MIS, respectively. It can be seen that theoretical q_e values obtained from pseudo second order model are very close to the experimental q_e values obtained. Therefore, these results predict that chemisorption is likely

Table 3
Adsorption rate constants (k_1 and k_2), maximum uptake at equilibrium (q_e) and R^2 values obtained from pseudo-first order and pseudo-second order kinetic model for Cs(I) and Sr(II).

System	q_e (mg/g) Experimental	Pseudo-first order			Pseudo-second order		
		k_1(1/min)	q_e (mg/g)	R^2	k_2 (g/mg·min)	q_e (mg/g)	R^2
IIS-Cs(I)	1.547	4.61×10^{-3}	1.086	0.932	7.01×10^{-3}	1.872	0.996
MIS-Cs(I)	1.066	6.91×10^{-3}	1.022	0.995	1.29×10^{-2}	1.172	0.998
IIS-Sr(II)	0.630	4.60×10^{-3}	1.446	0.956	3.20×10^{-2}	0.659	0.994
MIS-Sr(II)	0.574	4.61×10^{-3}	1.522	0.971	3.52×10^{-2}	0.601	0.996

to be involved as the rate controlling step for the removal of these two radio toxic ions using IIS and MIS [65,66].

3.3.4. Competition adsorption with heavy metal ions and effect of ionic strength

The removal behaviour of these radio toxic ions in presence of various heavy metal ions such as Cd(II), Cu(II), Mn(II), Pb(II) and Sr(II)/Cs(I) were evaluated and the results are given in Figs. 10 a,b. The initial concentrations were maintained at 10.32 and 6.64 mg/L for Cs(I) and Sr(II), respectively. The concentration of heavy metal ions were 50 mg/L and the solution pH was 5.0. As shown in Fig. 10a, the presence of various heavy metal ions in excess significantly decreased the adsorption of Sr(II) using both IIS and MIS solids. However, Cs(I) removal by IIS was relatively higher even in the presence of these toxic heavy metal ions but the Cs(I) adsorption by MIS was greatly inhibited. It was observed that the Sr(II) removal in presence of Cd(II), Cu(II), Mn(II), Pb(II) and Cs(I) achieved at least ~20% or more using IIS or MIS. A significant decreased in the removal of Cs(I)by MIS and Sr(II) by IIS/MIS might be due to high affinity of these adsorbents towards divalent heavy metal ions. Previuosly, it was reported that divalent heavy metal ions (i.e., Cu(II) and Pb(II)) were predominantly bound by the strong forces and form the inner sphere complexes onto the surface of manganese modified natural sand [29]. Meanwhile, the effect of ionic strength studies indicate that Cs(I) and Sr(II) are weakly bound through electrostatic attraction and form outer sphere complexes on the surfaces of IIS and MIS. Therefore, due to this different behavior, the removal of Cs(I) and Sr(II) using MIS are greatly inhibited by the presence of heavy metal ions. On the other hand, the iron oxide nanoparticle immobilized sand showed specific adsorption for Cu(II), whereas the non-specific adsorption was observed for Cd(II) and Pb(II) [30]. As shown in Fig. 10a, the Cu(II) showed more negative effect on the removal of Cs(I) by IIS.

Furthermore, the effect of ionic strength in the removal of Cs(I) and Sr(II) were conducted by increasing the concentration of $NaNO_3$ from 0.001 to 0.1 mol/L. The initial concentration of Cs(I) and Sr(II) are 10.5 and 7.8 mg/L respectively, and the solutions pH were maintained at 5.0. It was observed that an increase in ionic strength of the solution significantly inhibit the removal of Cs(I) and Sr(II) by IIS and MIS. For Cs(I), the presence of 0.005 mol/L $NaNO_3$ caused to decreased the percentage removal to half of its removal in absence of $NaNO_3$.Further, an increased in the ionic strength showed further decreased on the removal of Sr(II) compared to Cs(I). Therefore, the effect of ionic strength suggests that

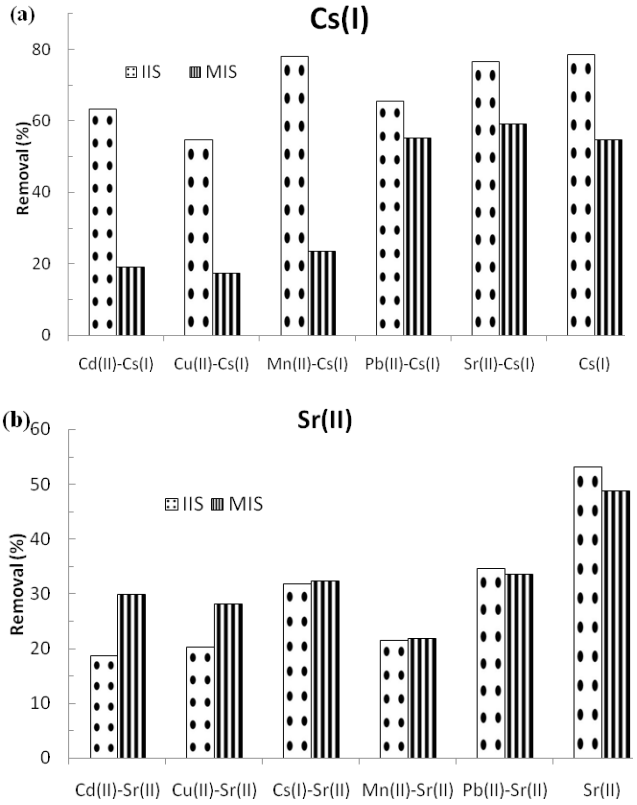

Fig. 10. (a) Effect of the presence of other metal ions on the adsorption of Cs(I) by IIS and MIS (Initial [Cs(I)]: 10.32 mg/L, pH: 5.0).(b) Effect of the presence of other metal ions on the adsorption of Sr(II) by IIS and MIS. (Initial [Cs(I)/Sr(II)]: 6.64 mg/L, pH: 5.0).

Cs(I) and Sr(II) are weakly bound to IIS/MIS forming outer sphere complexes. Previously, similar results were reported in which the removal of Sr(II) by potassium tetra-titanate and sodium trititanate were significantly decreased while increasing the NaCl or Na_2SO_4 concentrations from 0.001 to 0.012 mol/L [67]. Moreover, the presence of other competing ions such as Ca^{2+}, Na^+, K^+ and Mg^{2+}were reported to hinder the amount of Cs and Sr adsorption on moss [68].

3.4. Fixed-bed column adsorption study

Fixed-bed column experiments were performed using the initial concentration of 9.5 mg/Land 5.99 mg/L for Cs(I)

and Sr(II) respectively, and the break through curve are shown in Figs. 11a, b. This study showed that IIS and MIS solids could remove reasonable amount of Cs(I) and Sr(II) even under the dynamic conditions. The loading capacity of the columns containing IIS and MIS were optimized by modelling the breakthrough data with the non-linear Thomas equation [Eq. (5)] [69]:

$$\frac{C_e}{C_o} = \frac{1}{1 + e^{(K_T(q_o m - C_o V))/Q}} \quad (5)$$

where q_o is the loading capacity (mg/g) of the column packed with IIS and MIS; m denotes the mass of adsorbent (g) loaded in the column; C_e denotes the Cs(I)/Sr(II) concentration in the effluent (mg/L), where as C_o denotes the Cs(I)/Sr(II) concentration in the feed (mg/L); K_T represent the Thomas rate constant (L/min/mg); V represent the volume (L) of solution passing through the column; and Q represent the flow rate (L/min). The breakthrough data collected for Cs(I) and Sr(II) are fairly fit well to non-linear Thomas equation. The loading capacities (q_o) of the column as well as Thomas constants (K_T) were evaluated. The values obtained for q_o and K_T are summarized in Table 4. It was observed that the loading capacity obtained for Cs(I) were relatively higher than that obtained for Sr(II)using IIS and MIS. These findings agreed with the results obtained from batch adsorption studies. The adsorption capacity obtained under fixed-bed column system was relatively low comparing to batch system which is due to less contact time between the Cs(I)/Sr(II) and the IIS and MIS solids in fixed bed adsorption system [29].

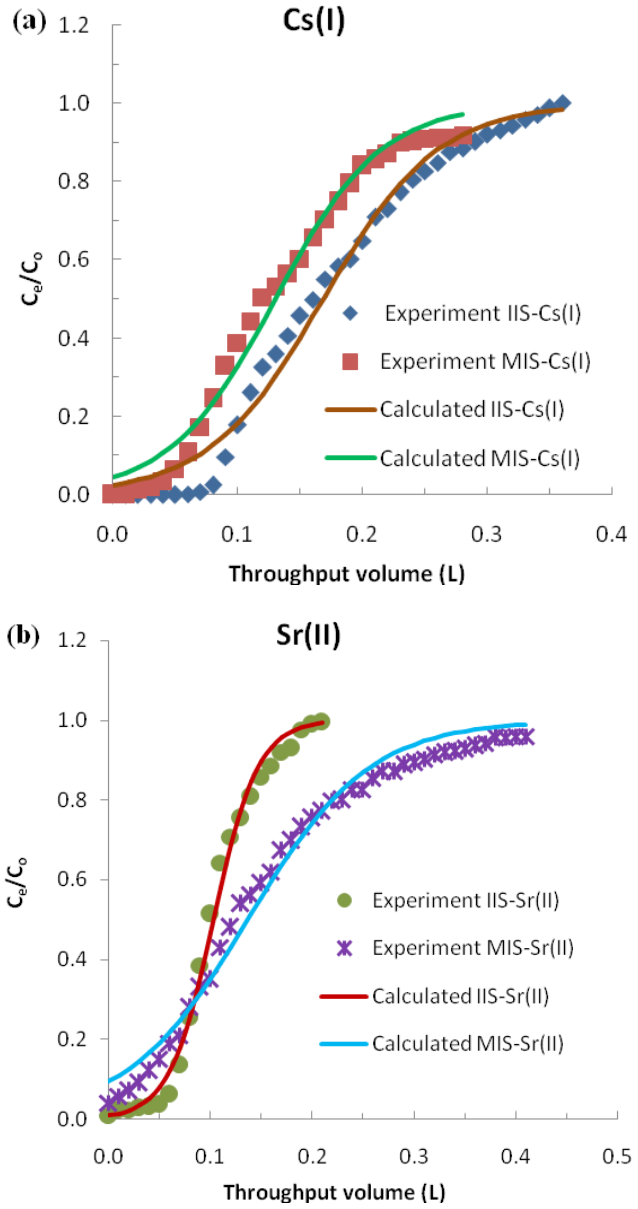

Fig. 11. Breakthrough curves of (a) Cs(I) and (b) Sr(II) adsorption using IIS and MIS.

4. Conclusions

Naturally available sand was modified by simple impregnation process to obtain iron oxide immobilized sand (IIS) or manganese oxide immobilized sand (MIS). The amount of iron and manganese loaded on the sand as evaluated by USEPA 3050B method were estimated to be 4.52 mg/g and 1.57 mg/g, respectively. The modified sand samples along with bare sand were characterized by SEM-EDX, FT-IR and XRD analytical methods. The IIS and MIS were successfully employed for the efficient removal of Cs(I) and Sr(II) from aqueous media. Batch studies showed that increasing the pH,initial concentration and contact time significantly favoured the adsorption of these two radio toxic contaminants. The presence of high concentration of heavy metal ions inhibit the adsorption of Sr(II) by IIS/MIS, whereas the Cs(I) removal by IIS was less affected. The effect of ionic strength studies indicate that Cs(I) and Sr(II) are weakly bound through electrostatic attraction and form outer sphere complexes on the surfaces of IIS and MIS. The equilibrium adsorption data showed a better fit to Freundlich adsorption isotherms and the kinetic data fitwell to pseudo second order kinetic model. The Langmuir adsorption capacity of IIS were found to be 5.102 and 1.324 mg/g for Cs(I) and Sr(II), respectively; whereas the MIS showed 2.409 and 1.277 mg/g for Cs(I) and Sr(II),

Table 4
The loading capacity and Thomas constants obtained for the removal of Cs(I) and Sr(II) using IIS and MIS

Materials	Cs(I)			Sr(II)		
	q_0(mg/g)	K_T(L/min/mg)	s^2	q_0(mg/g)	K_T(L/min/mg)	s^2
IIS	1.642	2.24×10^{-3}	7.2×10^{-2}	0.616	7.69×10^{-3}	2.5×10^{-2}
MIS	1.206	2.55×10^{-3}	5.1×10^{-2}	0.817	2.78×10^{-3}	5.5×10^{-2}

respectively. The breakthrough data were reasonably conform to Thomas equation and hence, the loading capacity of Cs(I) in the column packed with IIS and MIS were found to be 1.642 and 1.206 mg/g, respectively. The loading capacity of Sr(II) were slightly lower than Cs(I) and found to be 0.616 and 0.817 mg/g for the column packed with IIS and MIS, respectively. Therefore, this study indicate that the simple modified sand, i.e., IIS and MIS can be efficiently employed as potential adsorbent for the removal of radiotoxic Cs(I) and Sr(II) ions from aqueous solutions.

Acknowledgement

Following are results of a study on the "Leaders in INdustry-university Cooperation +" Project, supported by the Ministry of Education and National Research Foundation of Korea

References

[1] R. Kamaraj, S. Vasudevan, Evaluation of electro coagulation process for the removal of strontium and cesium from aqueous solution, Chem. Eng. Res. Des., 93 (2015) 522–530.
[2] K.-C. Song, H.K. Lee, H. Moon, K.J. Lee, Simultaneous removal of the radio toxic nuclides Cs^{137} and I^{129} from aqueous solution, Sep. Purif. Technol., 12 (1997) 215–227.
[3] D. Tiwari, Lalhmunsiama, S.I. Choi, S.M. Lee, Activated sericite: an efficient and effective natural clay material for attenuation of cesium from aquatic environment, Pedosphere, 24 (2014) 731–742.
[4] Y.K. Kim, K. Bae, Y. Kim, D. Harbottle, J.W. Lee, Immobilization of potassium copper hexacyanoferrate in doubly cross linked magnetic polymer bead for highly effective Cs^+ removal and facile recovery, J. Ind. Eng. Chem., https://doi.org/10.1016/j.jiec.2018.07.028
[5] T. Lan, Y. Feng, J. Liao, X. Li, C. Ding, D. Zhang, J. Yang, J. Zeng, Y. Yang, J. Tang, N. Liu, Biosorption behavior and mechanism of cesium-137 on Rhodosporidiumfluviale strain UA2 isolated from cesium solution, J. Environ. Radioact., 134 (2014) 6–13.
[6] C. Xiao, A. Zhang, Z. Chai, Synthesis and characterization of a novel organic–inorganic hybrid supra molecular recognition material and its selective adsorption for cesium, J. Radioanal. Nucl. Chem., 299 (2013) 699–708.
[7] M.R. Awual, S. Suzuki, T. Taguchi, H. Shiwaku, Y. Okamoto, T. Yaita, Radioactive cesium removal from nuclear wastewater by novel inorganic and conjugate adsorbents, Chem. Eng. J., 242 (2014) 127–135.
[8] L. Wu, G. Zhang, Q. Wang, L. 'an Hou, P. Gu, Removal of strontium from liquid waste using a hydraulic pellet co-precipitation micro filtration (HPC-MF) process, Desalination., 349 (2014) 31–38 .
[9] A. Zhang, C. Chen, E. Kuraoka, M. Kumagai, Impregnation synthesis of a novel macro porous silica-based crown ether polymeric material modified by 1-dodecanol and its adsorption for strontium and some coexistent metals, Sep. Purif. Technol., 62 (2008) 407–414.
[10] J. Pan, X. Zou, Y. Yan, X. Wang, W. Guan, J. Han, X. Wu, An ion-imprinted polymer based on palygorskite as a sacrificial support for selective removal of strontium(II), Appl. Clay Sci., 50 (2010) 260–265.
[11] Y. Wang, H. Huang, S. Duan, X. Liu, J. Sun, T. Hayat,A. Alsaedi, J. Li, A new application of a mesoporous hybrid of tungsten oxide and carbon as an adsorbent for elimination of Sr^{2+} and Co^{2+} from an aquatic environment. ACS Sustain. Chem. Eng., 6(2018) 2462–2473.
[12] S.V.S. Rao, B. Paul, K.B. Lal, S.V. Narasimhan, J. Ahmed, Effective removal of cesium and strontium from radioactive wastes using chemical treatment followed by ultra filtration, J. Radioanal. Nucl. Chem., 246 (2000) 413–418.
[13] S. Ding, Y. Yang, H. Huang, H. Liu, L. Hou, Effects of feed solution chemistry on low pressure reverse osmosis filtration of cesium and strontium, J. Hazard. Mater., 294 (2015) 27–34.
[14] M.V.B. Krishna, S.V. Rao, J. Arunachalam, M.S. Murali, S. Kumar, V.K. Manchanda, Removal of ^{137}Cs and ^{90}Sr from actual low level radioactive waste solutions using moss as a phyto-sorbent, Sep. Purif. Technol., 38 (2004) 149–161.
[15] A.G. Kotvitskyy, T.V. Maltseva, V.N. Belyakov, Selective removal of Cs^+ ions by means of electro-deionisation, Sep. Purif. Technol., 41 (2005) 329–334.
[16] C.C. Pavel, K. Popa, Investigations on the ion exchange process of Cs^+ and Sr^{2+} cations by ETS materials, Chem. Eng. J., 245 (2014) 288–294.
[17] S. Duan, X. Xu, X. Liu, Y. Wang, T. Hayat, A. Alsaedi, Y. Meng, J. Li, Highly enhanced adsorption performance of U(VI) by non-thermal plasma modified magnetic Fe_3O_4 nanoparticles, J. Colloid Interface Sci., 513 (2018) 92–103.
[18] D. Li, B. Zhang, F. Xuan, The sequestration of Sr(II) and Cs(I) from aqueous solutions by magnetic graphene oxides, J. Mol. Liq., 209 (2015) 508–514.
[19] M.W. Munthali, E. Johan, H. Aono, N. Matsue, Cs^+ and Sr^{2+} adsorption selectivity of zeolites in relation to radioactive decontamination, J. Asian Ceram. Soc., 3 (2015) 245–250.
[20] A. Dyer, J. Newton, M. Pillinger, Synthesis and characterisation of mesoporous silica phases containing heteroatoms, and their cation exchange properties. Part 3. Measurement of distribution coefficients for uptake of 137-Cs, 89-Sr and 57-Co radioisotopes, Micro porous Mesoporous Mater., 130 (2010) 56–62.
[21] S.G. Mashkani, P.T.M. Ghazvini, Biotechnological potential of *Azollafiliculoides* for biosorption of Cs and Sr: Application of micro-PIXE for measurement of biosorption, Bioresour. Technol., 100 (2009) 1915–1921.
[22] N.H.M. Kamel, Adsorption models of ^{137}Cs radionuclide and Sr (II) on some Egyptian soils, J. Environ. Radioact., 101 (2010) 297–303.
[23] Lalhmunsiama, D. Tiwari, S.-M. Lee, Physico-chemical studies in the removal of Sr(II) from aqueous solutions using activated sericite, J. Environ. Radioact., 147 (2015) 76–84.
[24] J. Li, X. Wang, G. Zhao, C. Chen, Z. Chai, A.Alsaedi, T. Hayatf , X. Wang, Metal–organic framework-based materials: superior adsorbents for the capture of toxic and radioactive metal ions, Chem. Soc. Rev., 47(2018) 2322–2356.
[25] H. Chen, D. Shao, J. Li, X. Wang, The uptake of radio nuclides from aqueous solution by poly(amidoxime) modified reduced graphene oxide, Chem. Eng. J., 254 (2014) 623–634.
[26] T. Štembal, M. Markić, N. Ribičić, F. Briški, L. Sipos, Removal of ammonia, iron and manganese from groundwaters of northern Croatia—pilot plant studies, Process Biochem., 40 (2005) 327–335.
[27] C. Lee, J. Jung, R. R. Pawar, M. Kim, Lalhmunsiama, S.M. Lee. Arsenate and phosphate removal from water using Fe-sericite composite beads in batch and fixed-bed systems. J. Ind. Eng. Chem., 47(2017) 375–383.
[28] Z. Sihaiba, F. Puleo, J.M. Garcia-Vargas, L. Retailleau, C. Descorme, L.F. Liotta, J.L. Valverde, S. Gil, A. Giroir-Fendler, Manganese oxide-based catalysts for toluene oxidation. Appl. Cat. B: Environ., 209 (2017) 689–700.
[29] D. Tiwari, C. Laldanwngliana, C.-H. Choi, S.M. Lee, Manganese-modified natural sand in the remediation of aquatic environment contaminated with heavy metal toxic ions, Chem. Eng. J., 171 (2011) 958–966.
[30] S.-M. Lee, C. Laldawngliana, D. Tiwari, Iron oxide nano-particles-immobilized-sand material in the treatment of Cu(II), Cd(II) and Pb(II) contaminated waste waters, Chem. Eng. J., 195–196 (2012) 103–111.
[31] S.A. Chaudhry , T.A. Khan, I. Ali. Adsorptive removal of Pb(II) and Zn(II) from water onto manganese oxide-coated sand: Isotherm, thermodynamic and kinetic studies. Egypt. J. Basic Applied Sc., 3 (2016) 287–300.
[32] S.A. Chaudhry, T.A. Khan, I. Ali, Equilibrium, kinetic and thermodynamic studies of Cr(VI) adsorption from aqueous solution onto manganese oxide coated sand, J. Mol. Liq., 236 (2017) 320–330.

[33] Y.-Y. Chang, K.-H. Song, J.-K. Yang, Removal of As(III) in a column reactor packed with iron-coated sand and manganese-coated sand, J. Hazard. Mater., 150 (2008) 565–572.
[34] Y. Cai, L. Li, H. Zhang, Kinetic modeling of pH-dependent antimony (V) sorption and transport in iron oxide-coated sand, Chemosphere., 138 (2015) 758–764.
[35] C. Varlikli, V. Bekiari, M. Kus, N. Boduroglu, I. Oner, P. Lianos, G. Lyberatos, S. Icli, Adsorption of dyes on Sahara desert sand, J. Hazard. Mater., 170 (2009) 27–34.
[36] R. Sanchis, J.A. Cecilia, M.D. Soriano, M.I. Vazquez, A. Dejoz, J.M. L. Nieto, E.R. Castellon, B. Solsona, Porous clays heterostructures as supports of iron oxide for environmental catalysis, Chem. Eng. J., 334 (2018) 1159–1168.
[37] X. Li, L. Zhang, H. Dong, T. Xia, Z. Huang, Bismuth oxide coated amorphous manganese dioxide for electrochemical capacitors, Solid State Sci., 43 (2015) 46–52.
[38] A. Bera, T. Kumar, K. Ojha, A. Mandal, Adsorption of surfactants on sand surface in enhanced oil recovery: Isotherms, kinetics and thermodynamic studies, Appl. Surf. Sci., 284 (2013) 87–99.
[39] T.A. Khan, S.A. Chaudhry, I. Ali, Thermodynamic and kinetic studies of As(V) removal from water by zirconium oxide-coated marine sand, Environ. Sci. Pollut. Res., 20 (2013) 5425–5440.
[40] T.A. Khan, S. Dahiya, E. A.Khan, Removal of direct red 81 from aqueous solution by adsorption onto magnesium oxide-coated kaolinite: isotherm, dynamics and thermodynamic studies, Environ. Prog. Sust. Energy, 36 (2017) 45–58.
[41] G. Anbalagan, A.R. Prabakaran, S. Gunasekaran, Spectroscopic characterization of indian standard sand, J. Appl. Spectrosc., 77 (2010) 86–94.
[42] G. Viruthagiri, S. Sathiyapriya, N. Shanmugam, A. Balaji, K. Balamurugan, E. Gopinathan, Spectroscopic investigation on the production of clay bricks with SCBA waste, Spectrochim. Acta. A. Mol. Biomol. Spectrosc., 149 (2015) 468–475.
[43] S.-M. Lee, Lalhmunsiama, S.-I. Choi, D. Tiwari, Manganese and iron oxide immobilized activated carbons precursor to dead biomasses in the remediation of cadmium-contaminated waters, Environ. Sci. Pollut. Res. Int., 20 (2013) 7464–7477.
[44] S. Skupiński, J. Solecki, Studies of strontium(II) sorption on soil samples in the presence of phosphate ions, J. Geochem. Explor., 145 (2014) 124–128.
[45] Z. Zhang, X. Xu, Y. Yan, Kinetic and thermodynamic analysis of selective adsorption of Cs(I) by a novel surface whisker-supported ion-imprinted polymer, Desalination., 263 (2010) 97–106.
[46] Y. Zhao, Z. Shao, C. Chen, J. Hu, H. Chen, Effect of environmental conditions on the adsorption behavior of Sr(II) by Na-rectorite, Appl. Clay Sci., 87 (2014) 1–6.
[47] Lalchhingpuii, D. Tiwari, S.I. Choi, Lalhmunsiama, S.M. Lee, Novel template synthesis and characterization of chitosan-silica composite: Evaluation of sorption characteristics of cadmium(II) and lead(II) by mesoporous chitosan-silica composite, Desal. Wat. Treat., 101 (2018) 232–241.
[48] V.B.H. Dang, H.D. Doan, T. Dang-Vu, A. Lohi, Equilibrium and kinetics of biosorption of cadmium(II) and copper(II) ions by wheat straw, Bioresour. Technol., 100 (2009) 211–219.
[49] T.A. Khan, M. Nazir, E.A. Khan, U. Riaz, Multi walled carbon nanotube-polyurethane (MWCNT/PU) composite adsorbent for safranin T and Pb(II) removal from aqueous solution: Bathc and fixed bed studies, J. Mol. Liq., 212 (2015) 467–479).
[50] I. Langmuir, The adsorption of gases on plane surfaces of glass, mica and platinum, J. Am. Chem. Soc., 40 (1918) 1361–1403.
[51] T.A. Khan, M. Nazir, Enhanced adsorptive removal of a model acid dye bromothymol blue from aqueous solution using magnetic chitosan-bamboo sawdust composite: batch and column studies. Environ. Prog. Sust. Energy, 34 (2015) 1444–1454.
[52] A. Ghaemi, M. Torab-Mostaedi, M. Ghannadi-Maragheh,Characterizations of strontium(II) and barium(II) adsorption from aqueous solutions using dolomite powder, J. Hazard. Mater., 190 (2011) 916–921
[53] T.A. Khan, M. Nazir, E.A. Khan, Magnetically modified multi walled carbon nanotubes for the adsorption of bismarck brown R and Cd(II) from aqueous solution: batch and column studies, Desal. Wat. Treat., 57 (2016) 19374–19390.
[54] S. Feng, X. Li, F. Ma, R. Liu, G. Fu, S. Xing, and X. Yue, Prussian blue functionalized micro capsules for effective removal of cesium in a water environment,RSC Adv., 6 (2016) 34399–34410.
[55] C. Jeon, Removal of cesium ions from aqueous solutions using immobilized nickel hexacyanoferrate-sericite beads in the batch and continuous processes, J. Ind. Eng. Chem., 40 (2016) 93–98.
[56] D. Ding, Y. Zhao, S. Yang, W. Shi, Z. Zhang, Z. Lei, Y. Yang, Adsorption of cesium from aqueous solution using agricultural residue – walnut shell: equilibrium, kinetic and thermodynamic mode-ling studies. Water Res., 47 (2013) 2563–2571.
[57] D. Ding, Z. Lei, Y. Yang, Z. Zhang, Efficiency of transition metal modified akadama clay on cesium removal from aqueous solutions. Chem. Eng. J., 236 (2014) 17–28.
[58] A.E. Ofomaja, A. Pholosi, E.B. Naidoo, Kinetics and competitive modeling of cesium biosorption onto iron(III) hexacyanoferrate modified pine cone powder,Int. Biodeter. Biodegr., 92 (2014) 71–78.
[59] A. Bouzidi, F. Souahi, S. Hanini, Sorption behavior of cesium on Ain Oussera soil under different physico chemical conditions, J. Hazard. Mater., 184 (2010) 640–646.
[60] M.Y. Miah, K. Volchek, W. Kuang, F.H. Tezel, Kinetic and equilibrium studies of cesium adsorption on ceiling tiles from aqueous solutions, J. Hazard. Mater.,183 (2010) 712–717.
[61] I. Smiciklas, S. Dimovic, I. Plecas, Removal of Cs^{1+}, Sr^{2+} and Co^{2+} from aqueous solutions by adsorption on natural clinoptilolite, Appl. Clay Sci., 35 (2007) 139–144.
[62] Z. Cheng, Z. Gao, W. Ma, Q. Sun, B. Wang, X. Wang, Preparation of magnetic Fe_3O_4 particles modified sawdust as the adsorbent to remove strontium ions, Chem. Eng. J., 209 (2012) 451–457.
[63] A.R. Kaveeshwar, P.S. Kumar, E.D. Revellame, D.D. Gang, M. E. Zappi, R. Subramaniam, Adsorption properties and mechanism of barium (II) and strontium (II) removal from fracking wastewater using pecan shell based activated carbon, J. Clean. Prod., 193 (2018) 1–13.
[64] R.R. Pawar, Lalhmunsiama, H.C. Bajaj, S.-M. Lee, Activated bentonite as a low-cost adsorbent for the removal of Cu(II) and Pb(II) from aqueous solutions: Batch and column studies, J. Ind. Eng. Chem., 34 (2016) 213–223.
[65] Y.-S. Ho, Review of second-order models for adsorption systems, J. Hazard. Mater., 136 (2006) 681–689.
[66] Y.S. Ho, G. McKay, Pseudo-second order model for sorption processes, Process Biochem., 34 (1999) 451–465.
[67] W. Guan, J. Pan, H. Ou, H., X. Wang, X. Zou, W. Hu, C. Li, X. Wu, Removal of strontium(II) ions by potassium tetratitanate whisker and sodium trititanate whisker from aqueous solution: Equilibrium, kinetics and thermodynamics, Chem. Eng. J., 167 (2011) 215–222.
[68] M.V.B. Krishna, S.V. Rao, J. Arunachalam, M.S. Murali, S. Kumar, V.K. Manchanda, Removal of ^{137}Cs and ^{90}Sr from actual low level radioactive waste solutions using moss as a phyto-sorbent, Sep. Purif. Technol., 38 (2004) 149–161.
[69] H.C. Thomas, Heterogeneous ion exchange in a flowing system, J. Am. Chem. Soc., 66 (1944) 1664–1666.